Supplemental Information for:

A novel interaction between RAD23A/B and Y-family DNA polymerases

Nicholas W. Ashton[1†‡], Nancy Jaiswal[2†§], Natália Cestari Moreno[1], Irina V. Semenova[2], Dana A. D'Orlando[1¥], Marcela Teatin Latancia[1], Justyna McIntyre[1||], Roger Woodgate[1]*, Irina Bezsonova[2]*

[1] Laboratory of Genomic Integrity, National Institute of Child Health and Human Development, National Institutes of Health, 9800 Medical Center Drive, Bethesda, MD 20892-3371, USA

[2] Department of Molecular Biology and Biophysics, UConn Health, Farmington, CT 06032, USA

* Correspondence should be addressed to:

Roger Woodgate. Tel: +1 301-435-0740, Email: woodgate@mail.nih.gov

Irina Bezsonova. Tel: +1 860-679-2769, Email: bezsonova@uchc.edu

† The authors wish it to be known that, in their opinion, the first two authors should be regarded as joint First Authors.

This document includes:

Present affiliations:

‡ Department of Radiation Oncology, Dana-Farber Cancer Institute, Boston, MA 02215, USA

§ Department of Pathology and Laboratory Medicine, Indiana University School of Medicine, Indianapolis, IN 46202, USA

¥ Arbor Biotechnologies, 20 Acorn Park Dr. Cambridge, MA 02140

|| Institute of Biochemistry and Biophysics, Polish Academy of Sciences, ul. Pawinskiego 5A, 02-106, Warsaw, Poland

Supplemental Figures

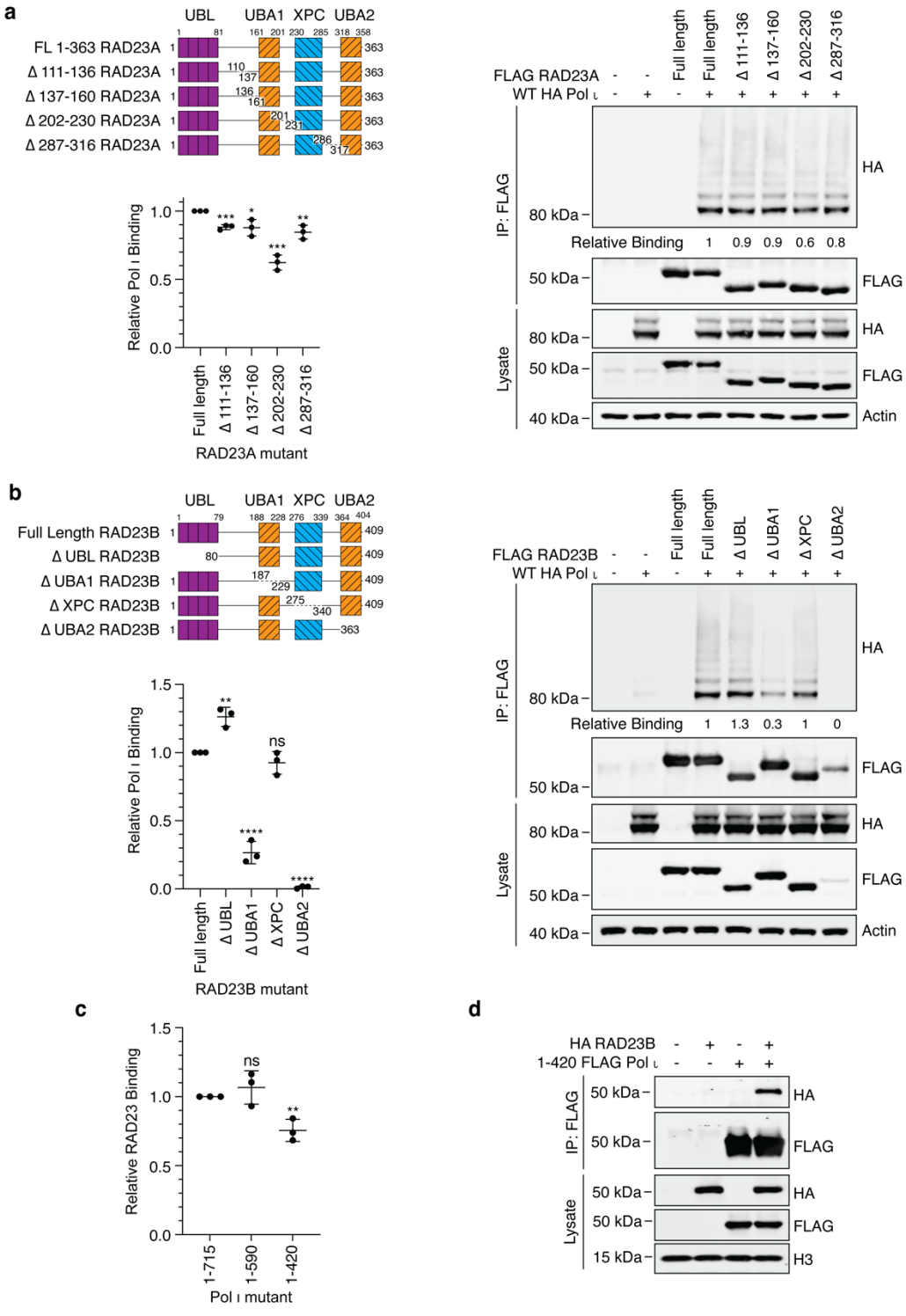

Supplemental Figure 1: UBA1 and UBA2 of the RAD23 proteins mediate an association with the catalytic domain of Pol ι. (**a - b**) The schematics represent FLAG-tagged RAD23A (above) and RAD23B (below) mutants used here. These mutants were immunoprecipitated from 293T cells co-expressing WT HA Pol ι. Eluent and whole cell lysate were immunoblotted as indicated. Relative binding was calculated based on the ratio of HA to FLAG proteins in the eluent. The bar graphs represent the quantification of relative binding from three repeats. Error bars represent standard deviation. Unpaired t-tests were used to assess whether there is a statistically significant difference in binding of Pol ι with the RAD23 mutants compared with the WT. ns = not significant, * = $p < 0.5$, ** = $p < 0.1$, *** = $p < 0.01$, **** = $p < 0.001$. (**c**) Bar graph representing the quantification of relative binding from three repeats of Figure 1c. Error bars represent standard deviation. Unpaired t-tests were performed as in (b). (**d**) Immunoprecipitation of 1-420 FLAG Pol ι from 293T cells co-expressing WT HA RAD23B. Eluent and WCL (input) were immunoblotted as indicated.

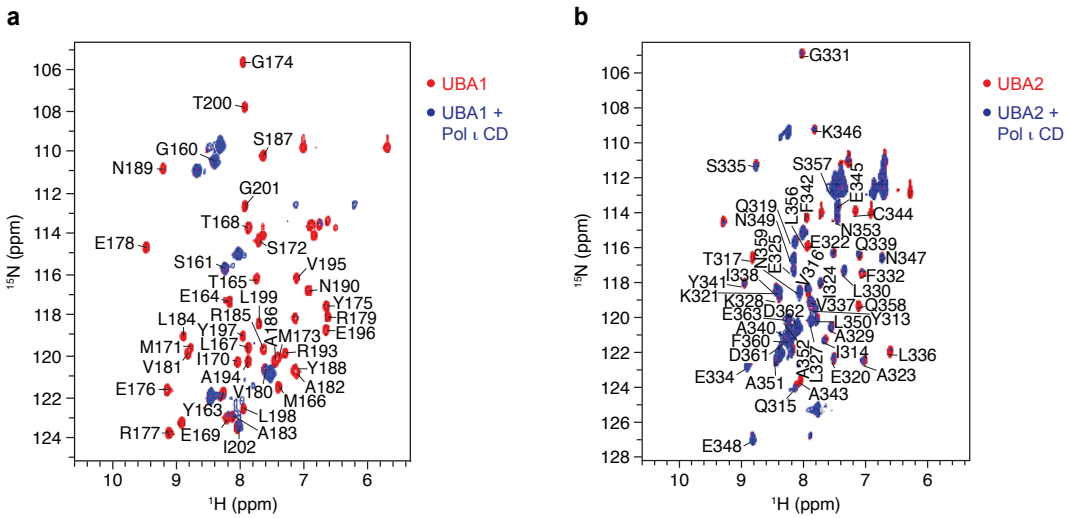

Supplemental Figure 2: UBA1 and UBA2 interact directly with the Pol ι catalytic domain. (**a - b**) 1H-15N HSQC spectrum of UBA1 (a) and UBA2 (b) when titrated with the Pol ι catalytic domain 1-419 (UBA1/UBA2 to Pol ι molar ratio = 1:1.2). Free and bound spectra have been shown in red and blue, respectively.

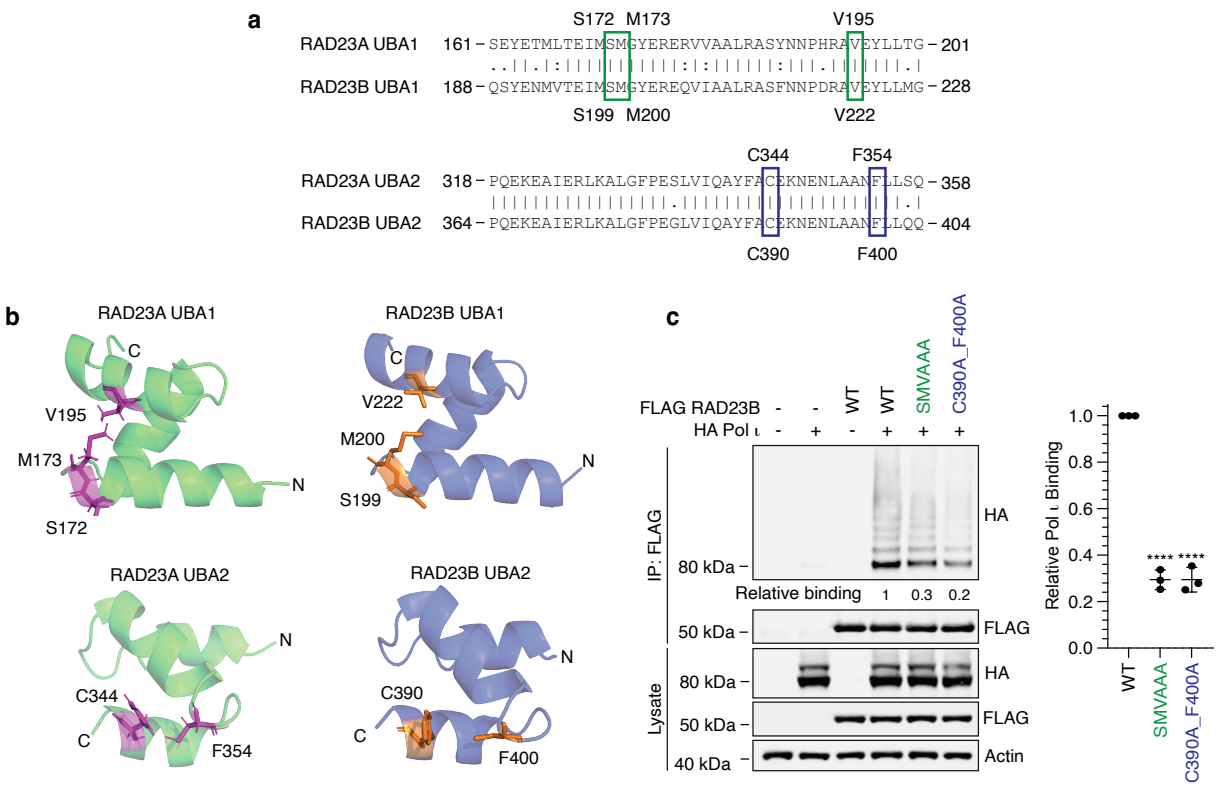
a
S172 M173
V195
RAD23A UBA1 161 – SEYETMLTEIMSMGYERERVVAALRASYNNPHRAVEYLLTG – 201
RAD23B UBA1 188 – QSYENMVTEIMSMGYEREQVIAALRASFNNPDRAVEYLLMG – 228
S199 M200
V222
C344
F354
RAD23A UBA2 318 – PQEKEAIERLKALGFPESLVIQAYFACEKNENLAANFLLSQ – 358
RAD23B UBA2 364 – PQEKEAIERLKALGFPEGLVIQAYFACEKNENLAANFLLQQ – 404
C390
F400
b
RAD23A UBA1
C
V195
M173
S172
N
RAD23B UBA1
C
V222
M200
S199
N
RAD23A UBA2
C344
C
F354
N
RAD23B UBA2
C390
C
F400
N
c
FLAG RAD23B - - WT WT SMVAAA C390A_F400A
HA Pol ι - + - + + +
IP: FLAG
80 kDa –
HA
Relative binding 1 0.3 0.2
50 kDa –
FLAG
Lysate
80 kDa –
HA
50 kDa –
FLAG
40 kDa –
Actin
Relative Pol ι Binding
1.0
0.8
0.6
0.4
0.2
0.0
****
****
WT
SMVAAA
C390A_F400A

Supplemental Figure 3: Point mutations in UBA1 and UBA2 of RAD23B disrupt binding to Pol ι. (**a**) Alignment of the amino acid sequences of UBA1 and UBA2 from RAD23A and RAD23B. Residues highlighted for UBA1 and UBA2 are those determined in Figure 4a as affecting the binding of Pol ι to RAD23A. (**b**) Ribbon structures of the RAD23A and RAD23B UBA1 and UBA2 domains, illustrating the position of amino acids highlighted in (a). The structures of RAD23A UBA1 [1] (PDB:1IFY) and UBA2 [2] (PDB:1DV0) were previously determined by solution NMR. The RAD23B structures are predictions generated by AlphaFold and available from the AlphaFold Protein Structure Database (available: https://alphafold.ebi.ac.uk/entry/P54727) [3, 4]. (**c**) Immunoprecipitation of the indicated RAD23B truncations from 293T cells co-expressing WT HA Pol ι. Eluent and WCL (input) were immunoblotted as indicated. Relative binding was calculated based on the ratio of HA to FLAG proteins in the eluent. The bar graph representing the quantification of relative binding from three repeats. Error bars represent standard deviation. Unpaired t-tests were used to assess differences in binding of Pol ι with WT vs mutant RAD23B WT. **** = $p < 0.001$.

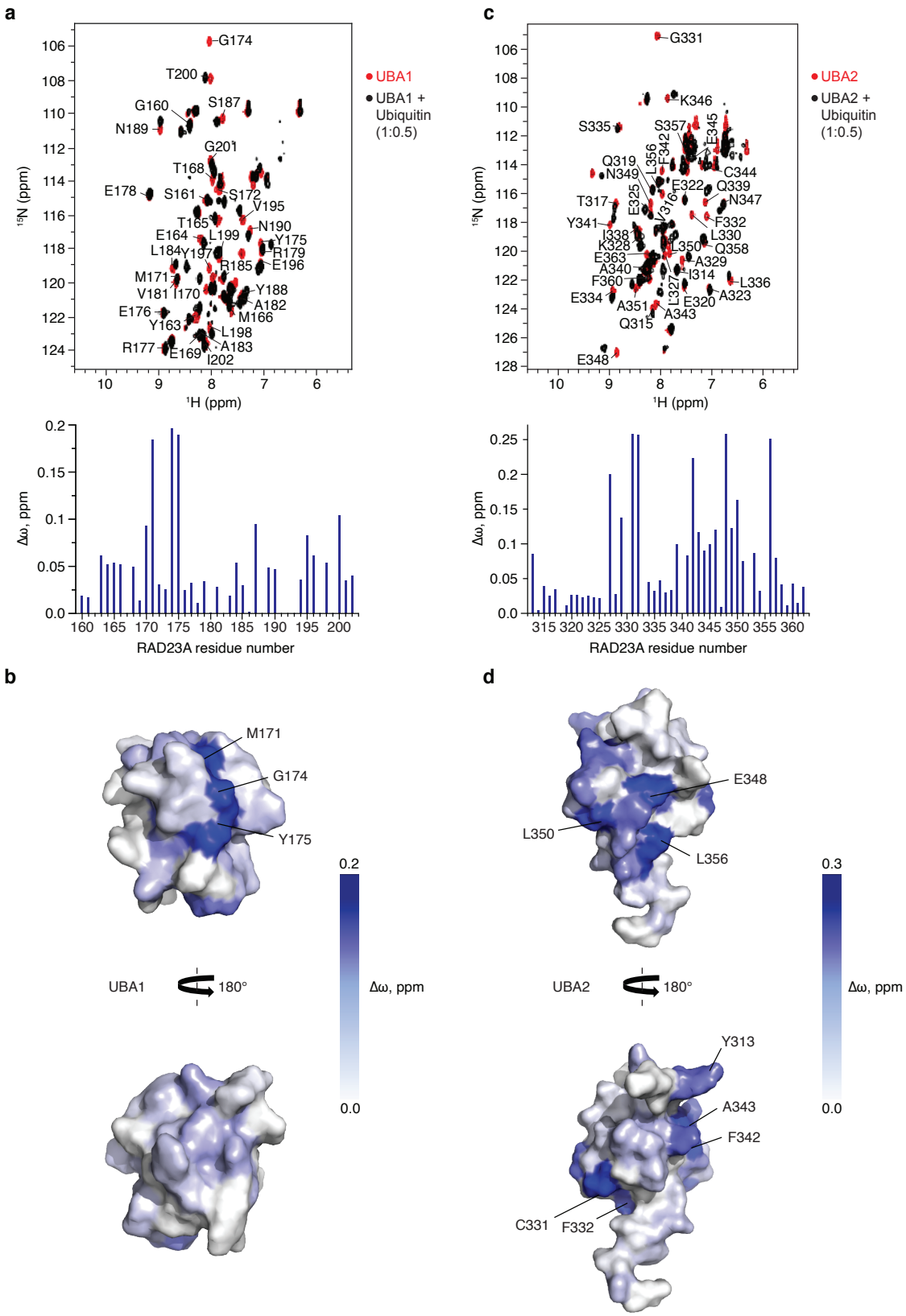
a
c
b
d
UBA1
UBA1 + Ubiquitin (1:0.5)
UBA2
UBA2 + Ubiquitin (1:0.5)
¹⁵N (ppm)
¹H (ppm)
Δω, ppm
RAD23A residue number
G174
T200
G160
S187
N189
G201
T168
E178
S161
S172
V195
T165
N190
E164
L199
Y175
L184
Y197
R179
R185
E196
M171
Y188
V181
I170
A182
E176
M166
Y163
L198
R177
E169
A183
I202
G331
K346
S335
S357
E345
Q319
N349
C344
E322
Q339
T317
N347
Y341
F332
I338
L330
K328
L350
Q358
E363
A329
A340
I314
F360
L336
E334
E320
A323
A351
A343
Q315
E348
M171
G174
Y175
UBA1
180°
0.2
0.0
Δω, ppm
E348
L350
L356
UBA2
180°
0.3
0.0
Δω, ppm
Y313
A343
F342
C331
F332

Supplemental Figure 4: UBA1 and UBA2 interact directly with ubiquitin (**a - b**) 1H-15N HSQC spectrum of UBA1 (a) and UBA2 (b) when titrated with ubiquitin. Free and bound spectra have been shown in red and black, respectively. Per-residue CSPs ($\Delta\omega$) due to ubiquitin binding were quantified and represented as bar plots. (**c - d**) Surface representation of the RAD23A UBA (c) and UBA2 (d) domains. CSPs from NMR experiments were used to map the binding interface, shown in blue.

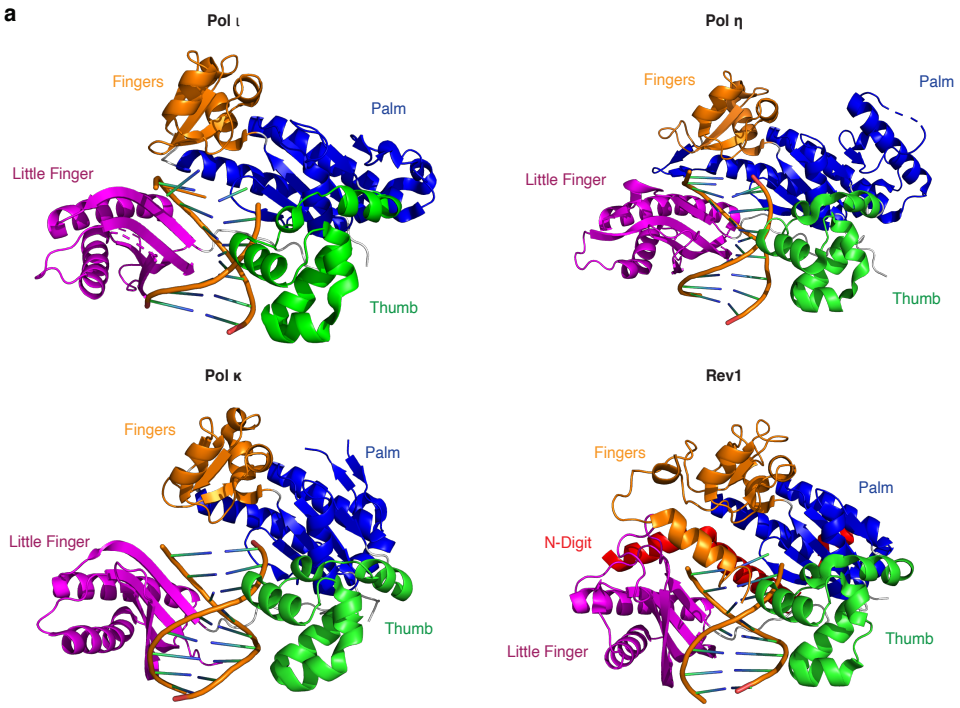
a
Pol ι
Fingers
Palm
Little Finger
Thumb
Pol η
Fingers
Palm
Little Finger
Thumb
Pol κ
Fingers
Palm
Little Finger
Thumb
Rev1
Fingers
Palm
N-Digit
Little Finger
Thumb

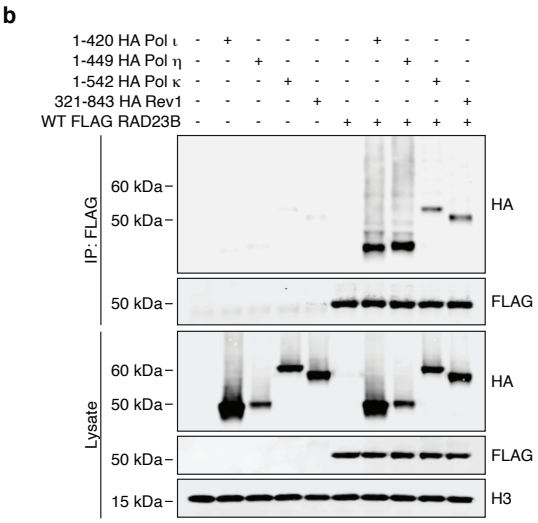
b
1-420 HA Pol ι - + - - - - + - - -
1-449 HA Pol η - - + - - - - + - -
1-542 HA Pol κ - - - + - - - - + -
321-843 HA Rev1 - - - - + - - - - +
WT FLAG RAD23B - - - - - + + + + +
IP: FLAG
60 kDa
50 kDa
HA
50 kDa
FLAG
Lysate
60 kDa
50 kDa
HA
50 kDa
FLAG
15 kDa
H3

Supplemental Figure 5. RAD23A and RAD23B binding the catalytic domains of each human Y-family DNA polymerases. (**a**) Ribbon illustrations of the crystal structures of the Pol ι (PDB:3GV8) [5], Pol η (PDB:4J9K) [6], Pol κ (PDB:6CST) [7] and REV1 (PDB:3GQC) [8] catalytic domains. Colors highlight the fingers, palm, thumb, and little finger sub-domains. (**b**) Immunoprecipitation of WT FLAG RAD23B from 293T cells co-expressing HA-tagged catalytic domains of Pol ι, Pol η, Pol κ and Rev1. Eluent and WCL (input) were immunoblotted as indicated.

Dataset 1 (separate file)

A dataset of proteins for which statistically significantly differences in signal intensity were observed between Pol ι and control treated ProtoArray microarrays. ProtoArrays were incubated with WT FLAG Pol ι, or a control solution, for 1 hour. Arrays were then washed and incubated with mouse anti-Pol ι primary antibodies, washed again, and incubated with Alexa647-conjugated anti-Mouse secondary antibodies. After a final wash, arrays were scanned, and fluorescent signal intensity quantitated. Magnitude change was calculated as log(SNR)Pol ι-treated - log(SNR)control to give an estimate of magnitude change. Data from the 2211 proteins for which statistically significantly differences in signal intensity were observed are presented here.

References

[1] Mueller TD, Feigon J. (2002). Solution structures of UBA domains reveal a conserved hydrophobic surface for protein-protein interactions. *J Mol Biol*. **319**, 1243-1255.

[2] Withers-Ward ES, Mueller TD, Chen IS, Feigon J. (2000). Biochemical and structural analysis of the interaction between the UBA(2) domain of the DNA repair protein HHR23A and HIV-1 Vpr. *Biochemistry*. **39**, 14103-14112.

[3] Jumper J, Evans R, Pritzel A, Green T, Figurnov M, Ronneberger O, Tunyasuvunakool K, Bates R, Zidek A, Potapenko A, Bridgland A, Meyer C, Kohl SAA, Ballard AJ, Cowie A, Romera-Paredes B, Nikolov S, Jain R, Adler J, Back T, Petersen S, Reiman D, Clancy E, Zielinski M, Steinegger M, Pacholska M, Berghammer T, Bodenstein S, Silver D, Vinyals O, Senior AW, Kavukcuoglu K, Kohli P, Hassabis D. (2021). Highly accurate protein structure prediction with AlphaFold. *Nature*. **596**, 583-589.

[4] Varadi M, Anyango S, Deshpande M, Nair S, Natassia C, Yordanova G, Yuan D, Stroe O, Wood G, Laydon A, Zidek A, Green T, Tunyasuvunakool K, Petersen S, Jumper J, Clancy E,

Green R, Vora A, Lutfi M, Figurnov M, Cowie A, Hobbs N, Kohli P, Kleywegt G, Birney E, Hassabis D, Velankar S. (2022). AlphaFold Protein Structure Database: massively expanding the structural coverage of protein-sequence space with high-accuracy models. *Nucleic Acids Res*. **50**, D439-D444.

[5] Kirouac KN, Ling H. (2009). Structural basis of error-prone replication and stalling at a thymine base by human DNA polymerase ι. *EMBO J*. **28**, 1644-1654.

[6] Zhao Y, Gregory MT, Biertumpfel C, Hua YJ, Hanaoka F, Yang W. (2013). Mechanism of somatic hypermutation at the WA motif by human DNA polymerase η. *Proc Natl Acad Sci U S A*. **110**, 8146-8151.

[7] Jha V, Ling H. (2018). 2.0 A resolution crystal structure of human polκ reveals a new catalytic function of N-clasp in DNA replication. *Sci Rep*. **8**, 15125.

[8] Swan MK, Johnson RE, Prakash L, Prakash S, Aggarwal AK. (2009). Structure of the human Rev1-DNA-dNTP ternary complex. *J Mol Biol*. **390**, 699-709.